

Direct and Indirect Searches for Dark Matter in the Form of Weakly Interacting Massive Particles (WIMPs)

Nader Mirabolfathi
University of California, Berkeley

ABSTRACT

Numerous lines of evidence indicate that the matter content of the Universe is dominated by some unseen component. Determining the nature of this Dark Matter is one of the most important problems in cosmology. Weakly Interacting Massive Particles (WIMPs) are widely considered to be one of the best candidates which may comprise the Dark Matter. A brief overview of the different methods being used to search for WIMP Dark Matter is given, focusing on the technologies of several benchmark experiments.

1 Introduction

The nature of dark matter is one of the oldest and most important open questions in cosmology, dating back to the first observations of anomalous high kinetic energies in distant galaxy clusters made by Swiss cosmologist Fritz Zwicky in 1933 [1]. Since then, exciting developments in observations of the cosmic microwave background (CMB), large-scale structure (LSS), and type Ia supernovae have allowed more accurate measurement of the various parameters of the “standard model of cosmology”. In particular, the Universe appears to be dominated ($\sim 70\%$) by the vacuum energy density, or Dark Energy, while the remainder ($\sim 30\%$) is made up of matter. Furthermore, most of the matter of the Universe appears to be non-luminous (i.e. dark) and non-baryonic. The nature of the Dark Matter is still unknown, and remains the subject of intense research activity. Weakly Interacting Massive Particles (WIMPs), a generic name for heavy particles interacting at the weak scale with baryonic matter, are among the best candidates which may comprise the Dark Matter. If such particles are produced thermally in the early universe, their weak-scale couplings explains why their relic density is of the order of critical density today. Independently, supersymmetry theories predict a stable s-particle state whose properties are very similar to the hypothetical WIMPs.

This paper is a brief review and update of different experiments aiming to detect Dark Matter in the form of WIMPs. The experiments described in this paper are not meant to be a complete list, but are selected to represent broader classes of the similar experiments.

2 Direct WIMP Searches

WIMPs can be detected either via (very rare) elastic scattering off the nucleus of ordinary matter (“direct detection”) or by measuring their annihilation products (“indirect detection”). The latter method is the subject of the section 3. In this section, the expected spectrum and rate of interaction of WIMPs with ordinary matter are estimated. After the experimental challenges for directly detecting WIMPs have been introduced, a brief review of the status and results from few important direct detection experiments will be presented.

WIMPs are expected to interact with the nucleons in ordinary matter [2]. The WIMP-nucleon elastic-scattering cross-section $\sigma_{\text{WIMP-p}}$ is SUSY model dependent [3]. One of the goals of all WIMP direct detection experiments is to determine or to limit $\sigma_{\text{WIMP-p}}$, and thus constrain the free parameter space available

for SUSY models. If the WIMPs are bound to the galaxy by the gravitational force, we can assume that their distribution should follow (Boltzman):

$$f(\vec{r}, \vec{v}, \vec{v}_E) = e^{-\frac{M_W(\vec{v}_E + \vec{v})^2 + M_W \Phi(\vec{r})}{k_B T}} \quad (1)$$

where M_W and T are the WIMP mass and the equivalent temperature ($kT = 1/2 M_W v_0^2$), $\Phi(\vec{r})$ is the local gravitational potential, v is WIMP velocity with respect to the earth, and v_E is the velocity of the Earth with respect to the center of the galaxy (sum of the Sun's velocity with respect to the center of the galaxy and the Earth's velocity with respect to the Sun):

$$v_E = 232 + 15 \cos 2\pi \frac{t - 152.5_{\text{days}}}{365.25_{\text{days}}} \quad [\text{km/s}] \quad (2)$$

Since the sinusoidal behavior comes from the Earth's motion around the sun, we expect its amplitude to be determined by the relationship between the Sun's velocity vector and the plane of the Earth's orbit. Thus we should expect an annual modulation of the WIMP flux of $\sim \pm 6\%$. The event rate is the product of the number of target nuclei (mN_0/A), the incoming flux of WIMPs, $v \cdot n$ (n determined by the eq. 1 from cosmology), and $\sigma_{\text{WIMP-p}}$ (predicted from the SUSY model in play). One could integrate over the WIMP velocity distribution and obtain the overall interaction rate. However, we are more interested in deriving the differential recoil energy spectrum. We will see that such a spectrum will directly give $\sigma_{\text{WIMP-p}}$ and the mass of the WIMPs. The recoil energy of a nucleus of mass M_T , which is hit by a WIMP of energy E , and which is recoiling at an angle θ , is given by:

$$E_R = E \frac{4M_W M_T}{(M_W + M_T)^2} \frac{(1 - \cos \theta)}{2} \quad (3)$$

Assuming a hard sphere scattering model (uniform E_R distribution) we can calculate the differential rate as:

$$\frac{\partial R}{\partial E_R} = \frac{R_0}{r E_0} \frac{2\pi^{3/2} v_0}{K} \int_{v_{\min}}^{v_{\text{esc}}} v e^{-\frac{(v+v_E)^2}{v_0^2}} dv \quad (4)$$

$$r = \frac{4M_W M_T}{(M_W + M_T)^2} \quad (5)$$

where $R_0 \sim n_0 v_0 \sigma_{\text{WIMP-p}}$, $E_0 = k_B T$, K is a normalization factor, v_{\min} is the minimum WIMPs velocity necessary to produce a recoil of E_R and v_{esc} is the galactic escape velocity. At the limit conditions ($v_e = 0$ and $v_{\text{esc}} = \infty$), eq. 4 becomes:

$$\frac{\partial R}{\partial E_R} = \frac{R_0}{rE_0} e^{-\frac{E_R}{rE_0}} \quad (6)$$

This form, although incorrect, illustrates the typical exponential behavior of the recoil energy spectrum. In particular, it shows that by observing the amplitude and the shape of the recoil energy spectrum, it is possible to constrain two physically important parameters: M_W and $\sigma_{\text{WIMP-p}}$.

So far, the discussion has been limited to zero-momentum transfer. When the momentum transfer $q = (2M_T E_R)^{1/2}$ is large enough so that the wavelength h/q is comparable to the size of the nucleus, coherence is lost and the cross section begins to decrease. This can usually be described by including a multiplicative form factor which depends on the type of WIMP-nucleon interaction (spin-dependent or spin-independent) as well as the nuclear structure: $\sigma(q^2) = \sigma_0 F^2(q^2)$. Figure 1 (left) shows the nuclear form factors calculated for various materials used in WIMP search experiments. Since different experiments use different target nuclei, it is preferable to report the recoil energy spectrum referred to nucleons (e.g. proton) rather than the nucleus, to allow easy comparison between experiments. If the WIMP-nucleon interaction is spin-independent, the contribution of various nucleons will be added coherently. Two corrections are important: The cross-section scales as $\mu_T = M_T M_W / (M_T + M_W)$ and the WIMP-nucleus coupling scales as A^2 . Hence,

$$\sigma_{\text{WIMP-Nucleus}} = \sigma_{\text{WIMP-p}} \frac{\mu_{\text{Nucleus}}^2}{\mu_p^2} A^2 \quad (7)$$

If the WIMP-nucleon cross-section is spin-dependent, WIMP-nucleon amplitudes still add coherently but the contributions of spin-paired nucleons will cancel each other. It is clear that the A^2 factor usually makes the spin-independent interaction dominant over the spin-dependent. We can now summarize these descriptions in a single equation:

$$\left. \frac{\partial R(v_e, v_{esc})}{\partial E_R} \right|_{(T, q^2)} = \left. \frac{\partial R(v_e, v_{esc})}{\partial E_R} \right|_{(p, 0)} \times F^2(E_R) \times S \quad (8)$$

where the (T, q^2) subscripts denote the WIMP interaction with the target nucleus at non-zero momentum transfer, $(p, 0)$ denote the same with the proton at zero momentum transfer, F^2 is the nuclear form factor, and S is the scaling factor (eq. 7).

Figure 1 (right) shows the expected rates on various materials for a 100 GeV/c² WIMP with $\sigma = 10^{-42}$ cm². Several important points are apparent from

these plots. First, the expected event rates are very low: Even for a 10 keV experimental energy threshold, one expects < 0.5 event/kg/day. Therefore, a very important goal of the direct detection experiments is to understand and to suppress various types of background. Second, due to the exponential nature of the spectrum, the majority of the signal is at very low energies. Therefore a low-energy threshold is essential. Third, despite the significant A^2 advantage of heavy nuclei (e.g. Xe), the nuclear form factor (Figure 1 left) suppression makes them less optimal at $E > 20$ keV. Therefore, Xe-based experiments would be more advantageous only if they could decrease the experimental threshold very low (which is not easy, as described later in this paper).

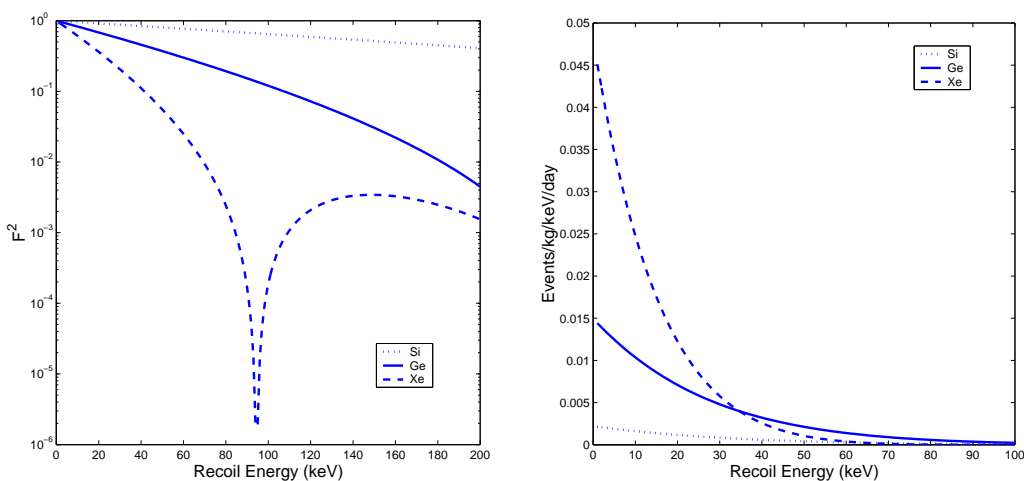


Figure 1: *On the left:* Nuclear form factors for Xe (dashed), Si (dots), Ge (solid). *On the right:* Differential recoil-energy spectra for Si (dots), Ge (solid), Xe (dashed)[4].

Thus the main goal of a WIMP search experiment is to produce detectors with extremely low background and very low threshold (< 15 keV) using materials with the best sensitivity to WIMPs. Due to the small interaction cross-section, a high mass - or, more accurately, a high exposure ($M \times T$) - is desirable. This can be obtained using large detector masses and long exposure times. This requires a high stability of the readout system (in particular, readout threshold) to various environmental conditions.

Currently we can classify direct WIMPs search experiments into two different categories: The first category, the first developed historically, focuses on building a detector with high mass and to passively reduce background by shielding the detector active region at deep underground sites. The hope is that after long exposures the sensitivity to the WIMP signal rises above background and eventually one can

hope to detect the cosmological signature (eq. 2). However, because the signal-to-background discrimination is of statistical nature, the sensitivity of this method only increases with $(M \times T)^{1/2}$. As representatives of this category of experiments, we discuss in more detail DAMA-NaI and ZEPLINI in the following sections. The second category of direct WIMP search experiments focuses mainly on an event-by-event discrimination of signal against background. As described at the beginning of this chapter, WIMPs interacting with the nucleus cause nuclear-recoils while most of the radioactive background (electromagnetic interaction) interact with electrons, giving electron-recoils. It has been shown (see section 2.3) that with a proper detector design one can distinguish the two types of events with a very high efficiency. Compared to the first category of experiments, the sensitivity is now enhanced in direct proportion to the exposure. As we will see, the experiments using this method obtained the best WIMP sensitivities.

2.1 DAMA

The DAMA project was begun in 1990 by an Italian group at Gran Sasso underground laboratory [5]. This elegant project is based on highly radiopure NaI(Tl) scintillator detectors shielded rigorously from radioactive background. The scintillation properties of NaI have been studied extensively for nuclear physics instruments. In particular, it has been shown that nuclear-recoil events can produce scintillation photons. It is possible to purify the crystals to achieve very low levels of background. The scintillation-yields are fairly low (0.3 for Na and 0.09 for I), leading to a recoil-energy threshold of ~ 20 keV for I, which is the more interesting nucleus for the WIMP-search due to its large A^2 factor. The group also showed that there is a slight difference between the pulse shapes produced by nuclear-recoil events and those produced by electron-recoil events. Though the latter factor could help to statistically discriminate WIMPs against radioactive background, it has been ignored in the DAMA data analysis due to low efficiency.

The DAMA experiment is placed among the first category of dark matter experiments (see the end of section 2), which require a large detector exposure (107,731 kg-day over 7 years of operation). If WIMPs form a halo embedding our galaxy, as the Sun is moving through the WIMP halo, the Earth should feel a wind of WIMPs with strength a function of its position in its orbit. Hence, one would expect to observe an annual modulation of the interaction rates. In 2000, using a five-year exposure, the DAMA collaboration claimed to observe a 6.3σ C.L annual modulation in WIMP-proton elastic scattering. Recently, DAMA confirmed the

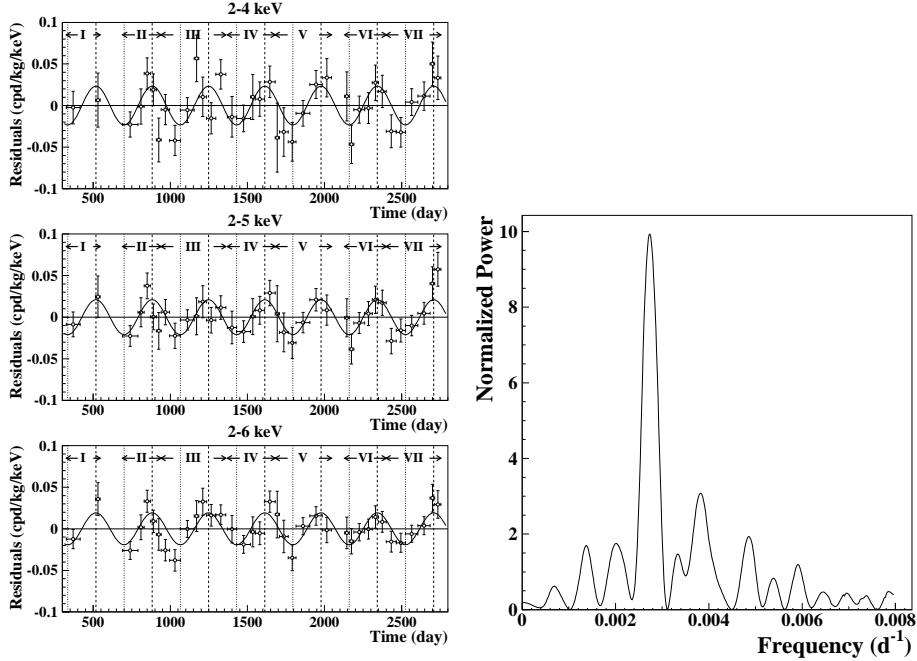


Figure 2: *On the left:* The DAMA experiment’s annual modulation of the residual rate (total rate minus constant) in the (2-4), (2-5), and (2-6) keV energy intervals as a function of the time over 7 annual cycles (total exposure 107731 kg × day); end of data taking July 2002. *On the right:* Power spectrum of the measured (2-6) keV modulation; the principal mode corresponds well to a 1 year period [6].

observation [6] by adding the results from two more annual cycles (Figure 2). While the DAMA evidence for the annual modulation is clear, its interpretation is more questionable. Most of the modulation signal comes from the lowest energy bins (2-6 keV), where understanding the efficiencies is particularly important. Although DAMA performed a study of the various possible systematic effects, some doubts remain that the signal may be caused by some other, less interesting, effects. The doubts are further fueled by the fact that there are three experiments (namely CDMS, Edelweiss, and ZEPLIN I) which have explored the same parameter space and found no signal.

Several upcoming experiments may help resolve the conflict: NaIAD (Boulby mine, UK)[7] has 65 kg of NaI crystals and is already acquiring data. ANAIS (Canfranc, Spain) [8] plans to use a detector mass of 107 kg of NaI, and has currently successfully tested a prototype. Both of these experiments should test the entire signal region claimed by DAMA in the coming 2-3 years.

2.2 Xe-based experiments

Liquid Xe can also be used to search for a direct WIMP signal. Xe has an obvious advantage over other materials due to its large A^2 ($A=131$) factor. However, as shown in Figure 1, this advantage is partially offset by the form factor suppression. Xe-based detectors would be particularly advantageous if their nuclear-recoil energy threshold can be reduced below 20 keV.

The signature of an interaction in Xe is twofold. First, there is electron excitation of Xe atoms, which leads to scintillation. Second, there is ionization of Xe atoms. The two signals can be used to discriminate against the electron-recoil events. In the absence of an electric field, the electron and ionized Xe recombine, producing secondary scintillation. The timing of the two scintillation pulses (nanosecond scale) differs for electron and nuclear-recoils, so pulse-shape discrimination can be used to suppress the electron-recoil background. This technique is used by ZEPLIN I (Boulby mine, UK) [9]. Their preliminary result is comparable with the Ge-based experiments CDMS (SUF) and Edelweiss, and incompatible with the signal region claimed by DAMA (Figure 4). However, these results are not based on an *in situ* neutron calibration.

Alternatively, an electric field may be used to extract the electrons of the ionization signal. Such techniques are being investigated for ZEPLIN II and ZEPLIN III (both at the Boulby mine, UK) [10]. Possibly the most important advantage of Xe detectors is their scalability to large detector masses. Such experiments (ZEPLIN IV and XENON [11]) are in the proposal stage. However, the dependence of the basic parameters, the ionization-yield and the scintillation-yield, on the energy and on the type of recoil are yet to be demonstrated.

2.3 Low temperature detectors: Solutions to event-by-event discrimination

The cryogenic calorimeters are, so far, the technologies best able to meet the two necessary requirements for a WIMP detector: Low threshold ($<10\text{keV}$) and good energy resolution ($<100\text{ eV}$). A cryogenic calorimeter consists of a dielectric crystal (Al_2O_3 , Ge, Si, CaWO_4 , etc.) cooled to temperatures as low as $0.01\text{ }^\circ\text{K}$. Because the heat capacity C of a crystal varies as $(T/\Theta_D)^3$, (Θ_D is the Debye temperature, e.g. $374\text{ }^\circ\text{K}$ for Ge) at very low T a small energy deposit from a particle interaction could significantly ($10^{-5}\text{ }^\circ\text{K}$) change the temperature of the absorber ($\Delta T = E/C$). A properly-attached thermometer (Mott-Anderson insulator or superconductor at its T_c) could thus measure the deposited energy. This is the best calorimetric measurement because all primary excitations due to the particle interaction will eventually

transform into thermal excitations. From another point of view, at very low temperatures the phonon (lattice vibration quanta) content of the crystal thermal bath is very low, and thus the out-of-equilibrium (athermal) phonons produced after an interaction may be easily distinguished and counted in order to measure the deposited energy. This combined with the fact that the excitation energy to create phonons is very low, $\sim 10^{-5}$ eV, compared to ~ 1 eV for conventional semiconductor detectors, makes cryogenic detectors the best calorimeters at low energies yet developed.

The above introduction suggests two distinct (but physically related) methods of calorimetric measurement. One method consists of measuring the detector temperature after it reaches the equilibrium state (at higher T of course) after the interaction. In this case, $\Delta T = E/C$ will directly measure the energy of the interacting particle. The second method, which requires a more elaborated readout system, is based on measuring the energy content of the athermal phonons created after an interaction, under the assumption that athermal phonons are proportionally produced and detected. As the athermal phonons carry information about the history of the event, the second method is more advantageous when it becomes important to reconstruct the history of an event in the detector. For example, it is often possible to reconstruct the location of an event in the detector, which in some cases is very important as we will see later in this paper. The signal amplitude in the first method depends on the mass of the detector as $C \propto M$, which limits the mass of the detectors. The second method does not suffer from this limitation, as long as the lifetime of the athermal phonons in the detector is longer than the response time of the readout system.

Calorimetric measurement alone is not enough to discriminate nuclear recoils (WIMPs) from electron-recoils (radioactive background), as the energy deposited does not depend on the type of interaction. However, it has been shown [12] that in semiconductor crystals (Ge, Si, etc.), the ionization-yield (charge/recoil energy) differs significantly between an electron-recoil and a nuclear-recoil. In Ge crystals, for example, the ionization-yield is 3 times bigger for an electron-recoil than for a nuclear-recoil. Figure 3 (left) shows the calibration results for one of the CDMS detector. Therefore, by simultaneously measuring ionization and phonons signal, one can obtain an event-by-event discrimination between a WIMP signal and the background. The CDMS and Edelweiss experiments use this method of detection and they are currently presenting the best sensitivities to WIMPs. This discrimination based on the ionization-heat measurement fails when an event occurs very close to the detector surface, in the “ionization dead-layer” [13]. The charge collection for such event could be incomplete, which could cause electron-recoil misidentification.

By measuring athermal phonons, CDMS is able to identify and reject events occurring very close to the surface based on timing parameters of the phonon pulse [14]. The Edelweiss experiment currently uses NTD-based heat sensors sensitive only to overall changes in temperature, and is unable to localize events in this manner. However, the group's recent studies of position-sensitive ionization-heat detectors look very promising [15],[16].

Scintillation-yield (light/recoil energy) could also differ between electron-recoils and nuclear-recoils. The CRESST experiment is based on simultaneous measurement of scintillation and ionization. There are also experiments, such as CUORE and CUORCINO [17], which are based on heat measurement alone. The complex techniques involved in low temperature devices make such detectors difficult to scale to large masses. The main challenge of the above mentioned experiments is to increase the mass of the detectors without compromising their sensitivity.

2.3.1 CDMS

CDMS uses ZIP (Z-dependent Ionization Phonon) detector technology to detect WIMPs [18]. ZIPs are disc-shaped (76 mm in diameter, 10 mm high) germanium or silicon crystals (absorber). One face of the disc is divided into four quadrants. Each quadrant is covered by a thin layer (350 nm) of lithographically-patterned aluminum fins (athermal phonon collectors) and 1024 tungsten transition-edge sensors ($1\mu\text{m} \times 250\mu\text{m} \times 35\text{nm}$ TES) which are evenly distributed over the surface. The Al layer is directly sputtered on the surface of the absorber ($> 80\%$ surface coverage) and provides a good phonon-phonon coupling between the two materials. The athermal phonons can pass the interface between the absorber and Al fins and directly relax their energy into the Al by breaking the Cooper pairs (creating quasi-particles) in the Al. These quasi-particles will tunnel into and become trapped in the TES's (tungsten $T_c \sim 0.07$ °K). The tungsten TES's are biased at the superconducting transition temperature, and thus a small variation in the TES temperature (due to the quasiparticle trapping) will cause a significant change in the TES resistance (~ 10 m Ω), which is then read out by a SQUID amplifier. The other face of the detector, which is also covered by aluminum, allows an electric field to be applied in order to collect the charge.

CDMS uses two methods to solve the near-surface event problem. First, an amorphous Si layer is introduced between the absorber and electrodes, which reduces the effect of near-surface trapping processes [13]. Second, the timing parameters of athermal-phonon signals can be used to identify the near surface events [14]. Figure

3 (right) shows the effectiveness of using athermal-phonon signal timing parameters in rejecting the near-surface events.

Each group of six Ge (250 g) or Si (100 g) detectors is packed in a single “tower” with their corresponding cold readout electronic instruments. Five “towers” are currently installed in a He₃ – He₄ dilution fridge (operating $T < 0.05$ °K) at Soudan underground laboratory. An overburden of 780 m of rock reduces the surface muon flux by a factor of $5 \cdot 10^{-4}$. Furthermore, the detectors are shielded against ambient radioactivity by ~ 0.5 cm of copper, 22.5 cm of lead, and 50 cm of polyethylene (to shield against neutrons). A 5-cm-thick scintillator muon veto enclosing the shielding identifies charged particles (and some neutral particles) that pass through it.

Recently, CDMS published [19] the analysis of its first Ge WIMP-search data (from the first “tower”) taken at Soudan during the period October 11, 2003 through January 11, 2004. After excluding time for calibrations, cryogen transfers, maintenance, and periods of increased noise, they obtained 52.6 live days with the four Ge and two Si detectors of “Tower 1”. This analysis revealed no nuclear-recoil events in 52.6 kg-d raw exposure in the Ge detectors. The data was used to set an upper limit on the WIMP-nucleon cross-section of $4 \cdot 10^{-43}$ cm² at the 90% C.L. at a WIMP mass of 60 GeV/c² for coherent scalar interactions and a standard WIMP halo (Figure 4). CDMS, which currently gives the best sensitivity to WIMPs yet attained, is now operating 2 detector towers (Tower 1+Tower 2) and plans to run 5 towers through the year 2005. The expected sensitivity reach for $\sigma_{\text{WIMP-nucleon}}$ is $\sim 3 \cdot 10^{-44}$ cm² based on 1200 kg-d projected exposure. Also a 99%-C.L. detection possibility is considered if $\sigma_{\text{WIMP-nucleon}} \sim 6 \cdot 10^{-44}$ cm².

2.3.2 *Edelweiss*

The Edelweiss experiment [20] is located at the LSM (French acronym for Modane Underground Laboratory). About 1700 m of rock protect the experiment from radioactive backgrounds generated by cosmic rays. In the laboratory, the muon flux is reduced by a factor $2 \cdot 10^{-6}$ compared to the flux at sea level. The experiment is surrounded by passive shielding made of paraffin (30 cm), lead (15 cm), and copper (10 cm). Edelweiss uses the same principle as CDMS for WIMP detection: Ionization-heat discrimination. Unlike CDMS’s athermal phonon sensors, the tiny rise in temperature due to a particle event is measured by an NTD (Neutron Transmutation Doped) heat sensor glued onto one of the charge-collection electrodes.

In 2000 and 2002, 11.6 kg-day were recorded with two different detectors

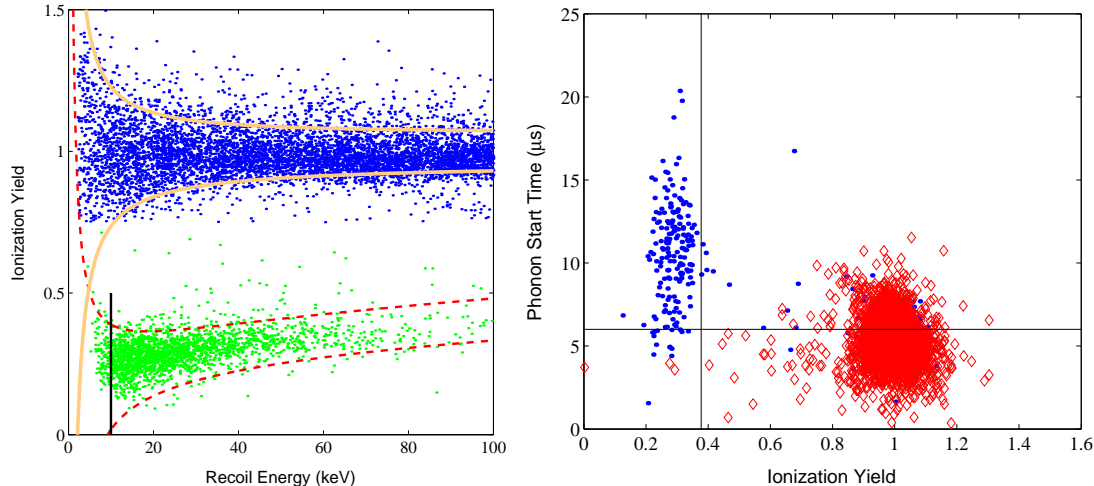


Figure 3: *On the left:* Ionization-yield versus recoil energy for a typical CDMS neutron (here with ^{252}Cf) and gamma calibration. Also shown on the figure are the $\pm 2\sigma$ nuclear-recoil band (dashed curve) and $\pm 2\sigma$ electron-recoil band (solid curve). *On the right:* Phonon start time versus ionization-yield for ^{133}Ba gamma-calibration events (diamonds) and ^{252}Cf neutron-calibration events (dots) in the energy range 20-40 keV in a typical CDMS detector. The diamonds that spread from yield=1 to yield=0.3 are near-surface events. Lines indicate typical timing and ionization-yield cuts, resulting in a high nuclear-recoil efficiency and a low rate of misidentified surface events[19].

[21]. In 2003, three new detectors were placed in the cryostat and 20 kg-day were added to the previous published data. Three events compatible with nuclear-recoils have been observed. However, the recoil energy of one of the events is incompatible with a WIMP mass $< 1 \text{ TeV}/c^2$. The two other events have been used to set the upper limit for WIMP-nucleon spin-independent interaction shown in Figure 4. The new limit is identical to the previous (11.7 kg-day), since the experiment is currently background-limited. The lack of an active surface-event rejection makes the distinction between nuclear-recoils and near-surface background events very difficult. Edelweiss is now implementing a new design based on NbSi thin-film Anderson insulator thermometers. The new detectors, which are sensitive to athermal phonons and have already demonstrated a high surface event rejection efficiency, will be functional during the Edelweiss II experimental stage [22].

As of March 2004, the Edelweiss I experiment has been stopped to allow the installation of the second-stage Edelweiss II. The aim is a factor of 100 improvement in sensitivity. A new low-radioactivity cryostat (with a capacity of 50 liters), able to

receive up to 120 detectors, is being tested in the CRTBT laboratory at Grenoble. The first runs will be performed with twenty-one 320 g Ge detectors equipped with NTD heat sensors and seven 400 g Ge detectors with NbSi thin film. With an improved polyethylene and lead shielding and an outer muon veto, the expected sensitivity for $\sigma_{\text{WIMP-nucleon}}$ is about 10^{-44} cm^2 .

2.3.3 Scintillation-heat : CRESST

The simultaneous detection of scintillation light and phonons in cryogenic calorimeters using scintillating absorber crystals can give a background suppression similar to that provided by the simultaneous measurement of ionization and light. Very recently it was shown [23] that a large variety of scintillating crystals (CaWO_4 , BaF , PbWO_4 , etc.) can be used in this manner. This gives this method a big advantage in identification of WIMP signals. The experiments using this technique are CRESST II and Rosebud. This technique has an important advantage over the Ge-based detectors in that it does not have surface-event problems. However, the technique also has some difficulties. First, rather than using PMTs to observe the scintillation signal (due to their high radioactive background), the current approach (taken by CRESST II [27]) is to use a second, phonon-mediated detector adjacent to the primary detector. The light collection is relatively poor, resulting in an energy threshold of 15-20 keV. Second, there are three nuclei in the crystal, all of which could potentially interact with the WIMPs. The scintillation-yield produced by the three nuclei has yet to be studied carefully, making event interpretation difficult. The goal of CRESST II is to build a 10 kg detector consisting of 300 g crystals to reach a sensitivity for $\sigma_{\text{WIMP-nucleon}}$ of the order of 10^{-44} cm^2 .

3 Indirect WIMP Searches

We now review the current state of the various WIMP indirect search methods. Indirect detection experiments search for products of WIMP annihilation in regions that are expected to have relatively large WIMP concentration. Examples of such regions are galactic centers, the center of the Sun, or the center of the Earth, where the WIMPs are expected to be gravitationally captured. Such searches assume that the WIMP is its own antiparticle (as predicted by SUSY models) or that equal numbers of WIMPs and anti-WIMPs are present. Higher WIMP density gives a larger annihilation signal, which can be manifested as a flux of γ -rays, neutrinos, or antimatter (positrons or anti-protons) produced in the WIMP-annihilation. We discuss these possibilities in some detail.

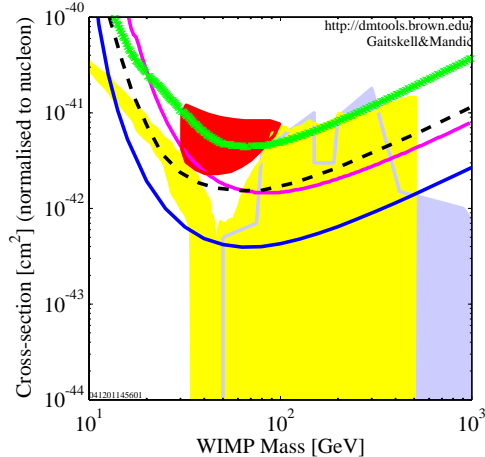


Figure 4: Limits on the WIMP-nucleon scalar cross section from CDMS[19] (solid blue), Edelweiss [20] (solid magenta), Zeplin I preliminary [24](dashed black), and CRESST (green crosses). Parameter above the curve is excluded at 90% C.L. These limits constrain several supersymmetry models, for example [26] (yellow) and [25] (blue). The DAMA 3σ signal region [6] is shown as a closed contour.

3.1 γ -rays

WIMP-annihilation can produce γ -rays in several different ways. First, a continuous spectrum is produced from the hadronization and decay of π_0 's produced in the cascading of the annihilation products. Second, γ -ray spectral lines are produced by the annihilation channels in which γ 's are directly produced, such as $XX \rightarrow \gamma\gamma$ (producing a line at M_X) and $XX \rightarrow \gamma Z$ (producing a line at $M_X(1 - M_Z^2/M_X^2)$). Observing such lines would be a clear detection of WIMP annihilation. Such γ -rays could be produced close to the galactic center. Although the production rates are relatively low, a large halo density may compensate sufficiently to make such signals observable.

Ground-based experiments rely on Atmospheric Cerenkov Telescopes (ACTs), which detect the Cerenkov light emitted by the shower produced by a γ -ray interacting at the top of the atmosphere. Some experiments, such as CELESTE (France) [28] and STACEE (New Mexico) [29], use the large mirrored areas used by solar power plants. These two experiments are sensitive to 20-250 GeV γ -rays. A number of experiments use dedicated mirrors or arrays of mirrors with a detector in the focal point: CANGAROO (Australia) [30], VERITAS (Arizona) [31], CAT (France) [32], HESS (Namibia) [33], HEGRA (Canary Islands, dismantled) [34], and MAGIC (Canary Islands) [35]. Such experiments are typically sensitive to 100 GeV - 10 TeV γ -rays. They are also capable of distinguishing (usually at $> 99\%$ efficiency) be-

tween the showers caused by γ -rays and those caused by cosmic rays (their dominant background). Finally, there are satellite-based experiments: EGRET [36] completed its mission and observed γ -rays in the 20 MeV - 30 GeV energy range, and GLAST [37] is scheduled to launch in 2006 and observe γ -rays of energies 10 MeV - 100 GeV.

Recently, two experiments have observed an excess flux of γ -rays coming from the galactic center. VERITAS [38], operating at the Whipple 10 m telescope on Mt. Hopkins, Arizona, observed an integral flux of $1.6 \pm 0.5 \pm 0.3 \cdot 10^{-8} \text{m}^{-2} \text{s}^{-1}$ with the energy threshold of 2.8 TeV. CANGAROO [39], with a lower threshold of 250 GeV, made a $\sim 10\sigma$ detection of the γ -ray source in the galactic center over the range 250 GeV - 2.5 TeV. However it is difficult to reconcile [40] the results of CANGAROO and VERITAS. The spectrum measured by CANGAROO is consistent with a WIMP mass of 1-3 TeV, while VERITAS, with its energy threshold of 2.8 TeV, requires a much heavier WIMP. Moreover, very high annihilation rates are required for this signal to be explained by WIMP annihilation. This implies very high annihilation cross-section and very high dark matter concentration at the galactic center. We note the possibility that these observations could also be explained by astrophysical sources, in particular the black hole at the galactic center. Results from the HESS experiment are expected in the near future - with four telescopes - HESS is expected to be more sensitive in the direction of the galactic center and to have superior angular resolution.

3.2 Neutrinos

Although WIMPs are expected to scatter very infrequently, they do scatter off of nuclei in the Sun or the Earth, lose, and become gravitationally bound. Hence, the density of WIMPs at the center of the Earth or the Sun can be considerably larger than in the halo, implying higher annihilation rates. Neutrinos produced in such WIMP-annihilations would penetrate to the Earth's surface, or escape from the Sun. The neutrinos can be produced both directly $XX \rightarrow \nu\bar{\nu}$ and indirectly $XX \rightarrow f\bar{f}$, where the fermion f can decay and emit a neutrino. Hence, the energy spectrum is expected to be continuous, rather than a line, but it is expected to extend up to the WIMP mass. If the neutrino interacts with rock sufficiently close to the Earth's surface, the products of the interaction may be detectable. The muon neutrinos are, hence, of the most interest, because their interactions produce muons which can travel considerable distance through the rock and reach a detector (electrons are absorbed at very short distances). The muon neutrinos can be detected at the surface of the Earth, usually using dedicated solar or atmospheric neutrino detectors.

In practice, one searches for upward-going muons - for the high-energy neutrinos, the muons produced are well-collimated with the original neutrino direction and carry much of the original neutrino's energy. Hence, one can search for the upward-going muon signal with a high-energy-threshold detector. The only known background are atmospheric neutrinos produced in the cosmic rays interactions with the atmosphere at the opposite side of the Earth.

Experiments designed to study solar or atmospheric neutrinos can also be used to look for the WIMP-annihilation neutrino signal. At the moment, none of the experiments has observed excess neutrinos from the Earth or the Sun, but several experiments have determined upper bounds on their flux: Baksan (neutrino experiment in Caucasus, Russia) [41], SuperKamiokande (atmospheric neutrino experiment in Japan) [42], MACRO (liquid scintillator neutrino experiment in Italy) [43], and AMANDA II (ice Cerenkov detector at the South Pole) [44]. These experiments are just beginning to probe the theoretically-allowed regions in supersymmetric WIMP models. Future experiments, such as ANTARES [45] and Lake Baikal [46], as well as future runs of AMANDA II and IceCube, are expected to improve the sensitivity to WIMP-annihilation neutrinos by ~ 2 orders of magnitude.

4 Conclusion

Direct detection experiments have already explored the regions of the most optimistic SUSY models. Despite their lower exposures (~ 50 kg-day, compared to 110,000 kg-day), event-by-event discrimination methods are currently giving the best sensitivities to the WIMP-nucleon scalar scattering cross-section. Extremely high discrimination combined with large mass seems to be the only solution for the next generation of direct detection experiments. The two-order-of-magnitude increase in the sensitivity of next-generation experiments will explore the core of many SUSY models in the next few years. Indirect detection will be complementary, but hardly competitive, for low- σ scalar WIMP detection. When combined with accelerator (LHC) results, the next generation of direct detection experiments may soon let us pinpoint the nature of the dark matter.

References

1. F. Zwicky, *Helv. Phys. Acta* **6**, 110 (1933).
2. M. Goodman and E. Witten, *Phys. Rev.* **D31**, 3059 (1985).
3. G. Jungman *et al.*, *Phys. Rep.* **267** (no 5-6), 195 (1996).

4. V. Mandic, First Results from the Cryogenic Dark Matter Search Experiment at the Deep Site, Ph.D. thesis, U.C. Berkeley, 2004.
5. P. Belli *et al.*, DAMA proposal to INFN Scientific Committee II, April 24 1990.
6. B. Bernabei *et al.*, astro-ph/0405282.
7. B. Ahmed *et al.*, Nucl. Phys. B Proc. Suppl. **124**, 193 (2003).
8. J. Morales *et al.*, Nucl. Phys. B Proc. Suppl. **118**, 525 (2003).
9. S. Hart, Nucl. Phys. B Proc. Suppl. **110**, 91 (2002).
10. D.B Cline, eConf C010630, E108 (2001).
11. E. Aprile *et al.*, astro-ph/0207670v1,31 Jul 2002.
12. T. Shutt *et al.*, Phys. Rev. Lett., 69(24), 3531 (1992).
13. T. Shutt *et al.*, Nucl. Inst. Meth. A **444**, 340 (2000).
14. V. Mandic *et al.*, Nucl. Instr. Meth. A **520**, 171 (2004).
15. N. Mirabolfathi *et al.*, AIP conference proceedings, Volume 605, 517 (2001).
16. S. Marnieros *et al.*, Nucl. Inst. Meth. A **520**, 185 (2004)
17. CUORE collaboration, Astropart. Phys. **20**, (2003) 91 (2003).
18. R. Clarke, An Athermal Phonon Mediated Dark Matter Detector with Surface Event Discrimination, Ph.D. thesis, Stanford Univ., 1999
19. CDMS Collaboration, Phys. Rev. Lett. **93**, 211301 (2004).
20. A. Benoit *et al.*, Phys. Lett. **B545**, 43 (2002).
21. A. Benoit *et al.*, Phys. Lett. **B530**, 15 (2001).
22. A. Broniatowstky *et al.*, AIP conference proceedings, Volume 605, 517 (2001).
23. N. Coron *et al.*, Proceedings of the Tenth International Workshop on Low Temperature Detectors, Genoa, July 2003, to appear in NIM A
24. V.A. Kudryavtsev, astro-ph/0406126
25. E.A. Baltz and P. Gondolo, Phys. Rev. **D67**, 063503 (2003).

26. A. Bottino *et al.*, Phys. Rev. **D69**, 037302 (2004).
27. M. Altmann *et al.*, astro-ph/0106314
28. <http://www.cenbg.in2p3.fr/extra/groupes/astrop/celeste.html>.
29. <http://www.astro.ucla.edu/stacee/index.html>.
30. <http://icrhp9.icrr.u-tokyo.ac.jp>.
31. <http://www.astro.ucla.edu/veritas>.
32. <http://lppn90.in2p3.fr/cat/index.html>.
33. <http://www.mpi-hd.mpg.de/hfm/HESS/HESS.html>.
34. <http://www.mpi-hd.mpg.de/hfm/CT/ctframestart.html>.
35. <http://hegra1.mppmu.mpg.de/MAGICWeb/>.
36. R. Hartman *et al.*, Astroph. J. Suppl. **123**, 79 (1999).
37. <http://www-glast.stanford.edu/>.
38. K. Kosack *et al.*, astro-ph/0403422.
39. K. Tsuchiya *et al.*, astro-ph/0403592.
40. D. Hooper *et al.*, astro-ph/0404205.
41. M. Boliev *et al.*, Proc. 24th ICRC (Rome) 1, 722 (1995).
42. S. Desai *et al.*, hep-ex/0404025.
43. M. Ambrosio *et al.*, Phys. Rev. **D60**, 082002 (1999).
44. J. Ahrens *et al.*, Phys. Rev. **D66**, 032006 (2002).
45. <http://antares.in2p3.fr/Overview>.
46. <http://www.ifh.de/baikal/baikalhome.html>.